A&A 412, 857–864 (2003)
DOI: 10.1051/0004-6361:20031479

Astronomy & Astrophysics

A measure of the network radiative properties over the solar activity cycle

I. Ermolli[1], F. Berrilli[2], and A. Florio[2]

[1] INAF – Osservatorio astronomico di Roma , Via Frascati 33, 00040, Monte Porzio Catone, Italia
[2] Dipartimento di Fisica, Università di Roma "Tor Vergata", Via della Ricerca Scientifica 1, 00133 Roma, Italia
e-mail: [berrilli; florio]@roma2.infn.it

Received 10 June 2003 / Accepted 3 July 2003

Abstract. Magnetic activity contributes to solar irradiance variations, both on short and long time scales. While sunspots and active region faculae are the dominant contributors to irradiance changes on time scales of days to weeks, the origin of the long term increase of the irradiance between activity minimum and maximum (≈0.1%) is still debated. It has been proposed that the small-scale magnetic elements composing the enhanced and quiet network take part substantially in this increase.
To contribute to this debate, we present the results obtained measuring changes in the radiative properties of the quiet network pattern along the current solar cycle. We use daily near simultaneous full-disk images provided by the Rome PSPT in three pass bands centered on CaII K line, blue and red Continua. The period analyzed ranges from July 1996 to September 2002, during the whole ascending phase of the current solar cycle.
We measured a network contrast change of about 0.05% in the two continuum PSPT bands and a network disk coverage change of the order of 6%. Under the simple hypothesis that network and quiet sun radiate as black bodies with the network at a slightly elevated temperature, the network contribution to TSI cycle variation, estimated over the period analyzed, is $\approx 3-4 \times 10^{-4}$.

Key words. Sun: photosphere – Sun: chromosphere – Sun: activity

1. Introduction

Space based measurements of the solar radiation integrated over the entire spectrum (Total Solar Irradiance, TSI), show clear rotational and solar-cycle variations, being about 0.1% higher during maximum activity conditions (see Fröhlich 2000 for a review). The modeling of this variability through comparison of spacecraft measurements of TSI with spatially resolved full-disk solar observations from both ground- and space- based instruments is now highly refined (Foukal & Lean 1988; Chapman et al. 1996; Fligge et al. 2000; Preminger et al. 2002; Jones et al. 2003; Krivova et al. 2003), with respect to the early modeling. The most recent results show that two classes of solar magnetic features, dark spots and bright faculae, account for about 90% of TSI variance, thus suggesting that solar magnetism is the primary cause of TSI variability during the solar cycle. However, none of these models has yet replicated the entire amplitude and detailed temporal behaviour of the observed solar irradiance variation. So, identification of the causes of residual variability in TSI is still necessary. Besides, the observation (de Toma et al. 2001) that TSI at the current solar maximum is very similar to that measured at the previous maximum, while solar activity indicators are lower in cycle 23 than in the previous one, suggests that more than solar activity is involved in TSI variations, as well as raising questions about the calibration accuracy of the space-based solar measurements.

Send offprint requests to: I. Ermolli,
e-mail: ilaria@mporzio.astro.it

A major portion of the long-term TSI variation is attributed to the changing emission of bright faculae and the magnetic network (Foukal & Lean 1988; Foukal et al. 1991). However, it has been shown that adjustments of the solar interior induced by variations of internal magnetic fields (Kuhn et al. 1998; Li & Sofia 2001), photospheric temperature changes (Kuhn et al. 1985, 1998) and radius changes (Ulrich & Bertello 1995; Sofia 1998) may also influence the long-term irradiance variation. Moreover, until recently the modeling of facular and network contributions to TSI variations suffered from uncertainties in observational determinations of the area, locations and contrasts of these bright magnetic features. These uncertainties are much larger for bright regions than for dark sunspots, so proxies of the facular and network brightening contribution to the TSI were used. These proxies (for example integrated CaII K flux, MgII index, 10.7 cm radio flux, He 1083 nm equivalent width), based on the observed close correlation between photospheric and chromospheric bright features in faculae and network, were converted to bolometric brightening by a careful regression against the observed irradiance adjusted for sunspot darkening (Willson & Hudson 1991; Harvey & Livingston 1994; Fröhlich 1994; de Toma et al. 1997; Fröhlich & Lean 1998). More recently, resolved space-based full-disk observations have been used, together with automated identification methods, to perform the data analysis with the aim of modeling the long-term TSI variation (Fligge et al. 2000; Krivova et al. 2003). However, these attempts are uncertain because of the need for a very careful analysis of the temporal change in the behaviour of the space-based instruments used to

get the observations (Ortiz et al. 2002b). While the main advantages of using space-based observations are the constant spatial resolution of the observations, no seeing degradation effects due to the Earth's atmosphere and the very well-known characteristics of the instrument and the data set, the accuracy of the calibration of the instrument degradation in space is certainly more difficult to determine than for ground-based instruments.

In order to contribute to the debate on residual long-term TSI variation, we attempt to measure changes in the photometric properties of the quiet network pattern along the current solar cycle. We used daily near-simultaneous full-disk images provided by the Rome PSPT in three bands. The PSPT has been developed by the National Solar Observatory in the framework of the NSF-promoted RISE (Radiative Inputs of the Sun to Earth) program, devoted to deepen the understanding of solar cycle irradiance variation. Both the instrument characteristics and the data calibration are carefully monitored. We studied the contrast and the disk coverage of the network pattern identified on full-disk images through automated procedures based on intensity thresholds and on skeletonizing algorithms. We studied the temporal dependence of these network properties during the ascending phase of Solar Cycle 23. We then used the results obtained to evaluate the network contribution to the TSI cycle variation measured from space, making the simple assumption that the continuum contrast variations measured over the disk are produced by a change in the brightness temperature of the corresponding parts of the Sun surface.

2. Observations and image pre-processing

2.1. Data archive

We analyzed images available from the data archive of the daily observations carried out with the PSPT telescope at the Rome Observatory, covering the period of observations from 1996 to 2002. The archive contains images taken by two iterations of the Rome PSPT telescope. The data from July 1996 to June 1997 were obtained by the PSPT prototype instrument. This instrument produced images with a 1024×1024 pixel, 12 bit/pixel CCD in the CaII K (393.3 ± 0.25 nm) and blue continuum (409.4 ± 0.25 nm). From October 1997 onwards, the data were obtained with the final version of the telescope, i.e. images were acquired with a 2048×2048 16 bit/pixel CCD camera, $2\times$ binned, with a final spatial scale of $\approx 2''$/pixel, using three interference filters centered on CaII K line (393.3 ± 0.25 nm), blue continuum (409.2 ± 0.25 nm) and red continuum (607.1 ± 0.5 nm).

The telescope was designed to provide high-precision photometric full-disk observations, utilizing a simple optical path to minimize scattered light contamination, an active mirror to reduce tracking errors and a high dynamic range "wide" camera. The PSPT concept and prototype are described in Coulter & Kuhn (1994) and Ermolli et al. (1998a,b). The current instrument operation is briefly described by Ermolli et al. (2001), with a more complete description available at `http://www.mporzio.astro.it/solare/eng/index_eng.html`

For the study presented here we selected from the full archive daily "triplets" of full-disk CaII K, blue and red images, obtained during 375 different observing days at Summer and Winter times (respectively, from July to September and from January to March), from 1996 up to 2002. We chose to analyze Summer time images because these were taken during better observing conditions (weather, timing, solar declination), while the Winter ones suffer worse observing condition effects.

All the images analyzed were obtained by co-adding frames acquired with very short exposure times (usually less than 50 ms). Each "triplet" of CaII K and continuum images were taken within few minutes (less than 5 min) to achieve near simultaneous observations of the solar photosphere and chromosphere.

2.2. Image pre-processing

The images in the Rome-PSPT archive are pre-processed to apply the instrumental calibration, i.e. corrected for dark current and flat field response. The flat-field image was obtained with the application of the "displaced image method" (Kuhn et al. 1991). This method uses a series of solar images, taken with the same optical system used to observe the Sun, with displacements of the solar disk center. We applied this method using 16 solar images with displacements ranging from a few to a few hundred pixels and a reference image with the solar disk centered on the CCD. On simulated images, the method recovers a known flat-field with accuracy better than one part in 10^4. This accuracy is required to resolve a temperature variation of amplitude 1 K from a black-body at temperature of 6000 K at a wavelength of 600 nm. The accuracy of the flat-field determination decreases up to 0.1−0.5% using real solar images, especially for those acquired under poor observing conditions (clouds, transparency variations, wind).

The analyzed images selected from the full archive were first processed to compensate for some observational effects. To compensate the scale image (there is a 0.6% and 2.5% difference in the disk size among CaII K, blue and red images) we shifted and re-sized the flat-fielded images with a linear interpolation (Fig. 1).

We removed the solar intensity limb darkening (CLV) from each image. We applied the circular intensity averaging method to the full-disk images (i.e. computation of the mean intensity of the quiet sun, avoiding active regions from the computation with an intensity threshold method), then we applied an ideal high-pass FFT filtering to correct for occasional modulations produced by the presence of active regions at the disk center. We normalized each image to its individual quiet Sun CLV dividing the relative intensities of the image by the computed CLV intensities (Fig. 2).

3. Image processing and network identification

In the first stage of the image processing we apply an image decomposition technique to identify and remove from each full-disk image the activity complexes. As we are interested in studying properties of the quiet network pattern on quiet Sun regions we used the technique proposed by Caccin et al. (1998). This technique differs, both in the approach and the data used, from several methods developed to separate in detail the activity structure in full-disk images. These methods include, for example, simple or complex threshold selection methods (Johannessen et al. 1995; Preminger et al. 2001), Gaussian

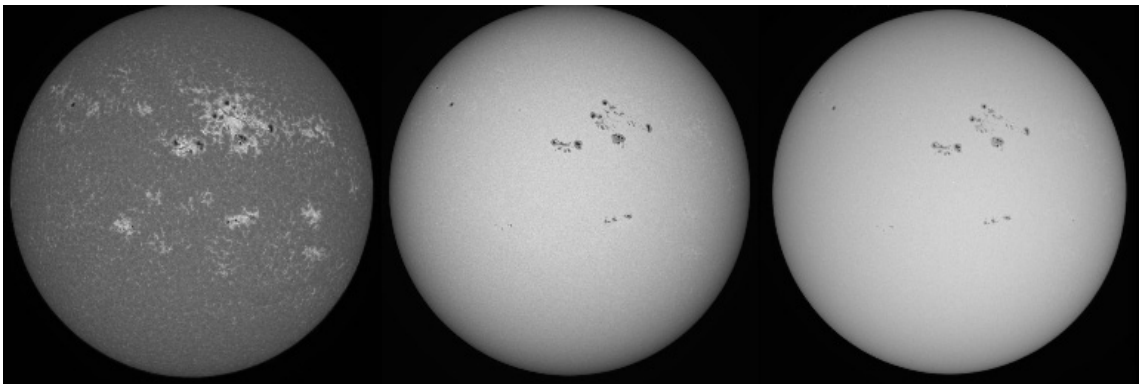

Fig. 1. An example of the PSPT images analyzed. From the left: CaII K, blue and red continuum images for July 29, 2002.

Fig. 2. An example of the results obtained by the processing applied to the images shown in Fig. 1. From left: CaII K image after removal of the center to limb variation, binary image produced by the active region and enhanced network masking, binary image with the identified network.

fits to full-disk residual intensity distributions (de Toma et al. 2001), statistical pattern recognition techniques (Turmon et al. 2002), and analysis of spatial patterns and structural properties in magnetograms, CaII K and continuum images (Worden et al. 1998; Harvey & White 1999). The Caccin et al. technique was developed principally to select quiet Sun regions from CaII K full-disk images. So, the technique takes into account intensity threshold and geometric connection criteria to compute redundant masks of the activity complexes and bright "extended" features identified over the disk.

There is no universally accepted, unique nomenclature for solar surface structures. We use the scheme of structure classes applied by Harvey & White (1999) to study magnetic structure properties by a decomposition of magnetograms and full-disk images. With respect to this scheme, regions masked by this technique include active and decaying active regions, as well as enhanced network elements.

Whenever activity complexes and enhanced network are identified, they are removed from the image. The intensity mean value computed for the quiet Sun is assigned to the pixels in all the identified regions, before proceeding to the network pattern identification.

The approach we used to identify the network is based on a skeletonizing iterative procedure, formally a Medial Axis Transform, applied to CaII K masked images. Particularly, the algorithm, following the ridges of connected CaII K bright features, points out the pixels belonging to the bright CaII K network. This network definition, not this segmentation procedure, is the same as that used by Hagenaar et al. (1997) to study the geometry of the supergranular chromospheric network. A complete description of this procedure and an exhaustive discussion of its general properties can be found in Berrilli et al. (1998, 1999b) and Florio & Berrilli (1998).

With respect to the procedure described in the papers cited we removed the thinning algorithm, aimed to study the morphological properties of supergranular cells, and we stick to the one-pixel wide identified pattern for all the pixels connected to pattern and with a contrast greater than the local average contrast. Therefore, at the end of the image processing we obtain a "thick skeleton" composed of connected, and not sparse, bright features that we "assume" to be representative of network pattern. In Fig. 2 we show an example of an original CaII K image with the corresponding identified network pattern at the end of our image processing.

4. Calculation of network properties

We define the network contrast in the three PSPT bands by the ratio between $I_{\rm Net}/I_{\rm quiet}$. $I_{\rm Net}$ is the average intensity of pixels identified by the skeleton and $I_{\rm quiet}$ is the average intensity of the quiet Sun area for each heliocentric position μ over the disk and each "triplet" of CaII K, blue and red Continua images. The network disk coverage α is calculated by the ratio between the number of pixels belonging to the identified network and the total number of pixels in the quiet Sun in the analyzed region-of-interest.

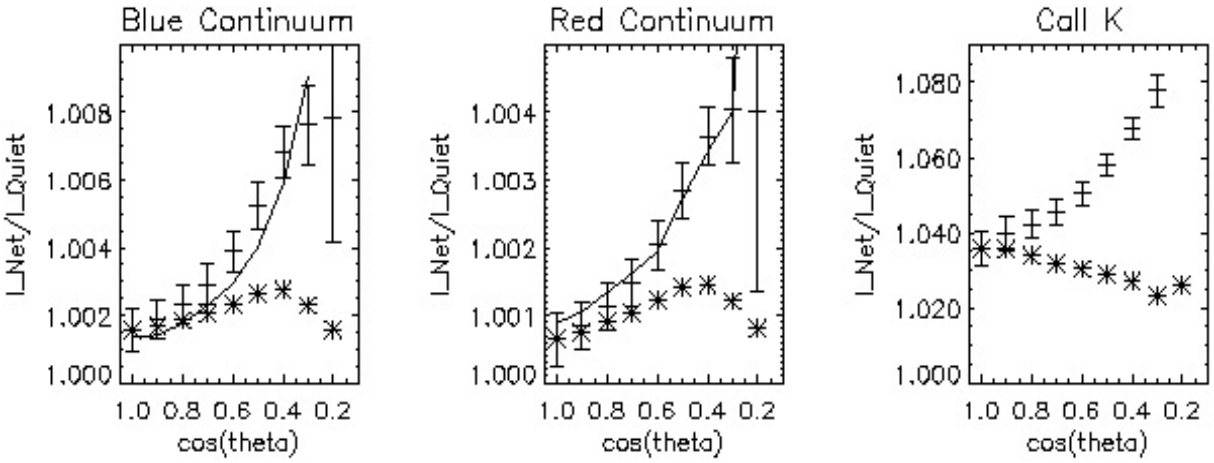

Fig. 3. Center to limb variation of the network contrast over the disk at the three PSPT bands (symbol) obtained analyzing the images acquired in 2001. The measured values (stars) were corrected for the geometrical projection effect at the various disk positions as described in the text. Comparison with the center to limb variation of the network contrast (line) obtained through a semiempirical atmospheric model of the network feature computed for the two continuum PSPT bands (Penza et al. 2003a). Bars represent the standard deviation of the mean in each bin.

4.1. Center to limb variation of the network contrast

In Fig. 3 we show the values of the network contrast measured over the disk for the three PSPT bands. We found a brightness excess of the network pattern with respect to the quiet Sun over the disk in the two continuum bands. The photospheric network contrast at the disk center are only a few tenths of a percent, slowly increasing toward the limb up to $\mu = 0.4$. The chromospheric network contrast at the disk center is a few units of a percent in the CaII K band, decreasing slowly near the limb as an effect of geometrical projection. At the different heliocentric positions, the contrast measurement of the very thin network feature becomes "corrupted" by a contribution from the quiet Sun that increases toward the disk limb. Taking into account this effect as described by Penza et al. (2003a), we obtained the "corrected" contrast values shown in Fig. 3. The contrast in the two continuum bands shows an high degree of linear correlation with $r = 0.994$. We found that the ratio of the blue to red contrasts is 1.0008 ± 0.0007.

4.2. Temporal variations of the network properties

We described the temporal variations of the network properties by analyzing the whole sample of full-disk images selected for the seven year period studied corresponding to the ascending phase of Solar Cycle 23. We found the variations of the network properties at the disk center shown in Fig. 4. Both the contrast and the disk coverage of the network slowly increase over the period analyzed. Note that the discontinuity of the results obtained for the two periods 1996−1997 and 1998−2002 arises from differences in the images analyzed due to inherent differences in the observational set-up utilized. Nevertheless, note the variation of the network radiative properties obtained by analyzing images taken since the final version of the PSPT telescope (late 1997).

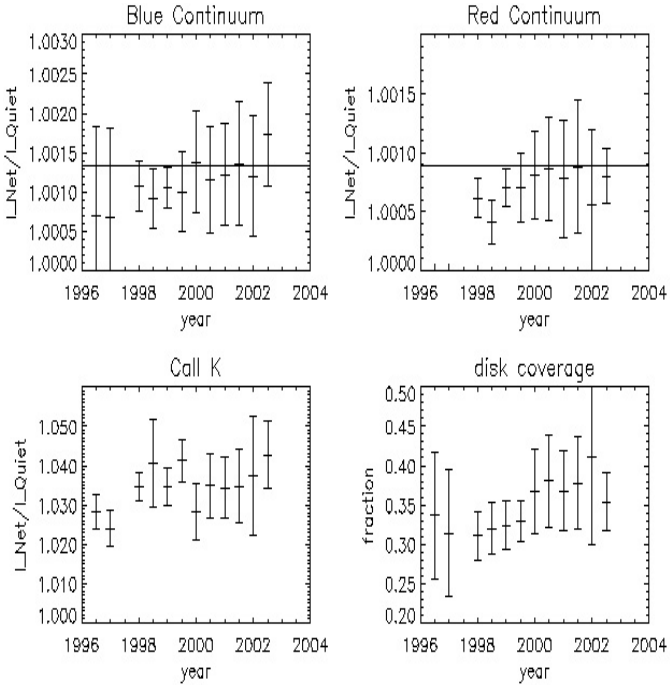

Fig. 4. Temporal variation of the network photometric properties over the period analyzed, spanning the ascending phase of Solar Cycle 23, from July 1996 to September 2002. Bars represent the variation of the values with respect to the mean. Comparison with the photometric properties (line) computed through a semiempirical atmospheric model of the network feature (Penza et al. 2003a). Bars represent the standard deviation of the mean in each bin.

5. A simple evaluation of the network contribution to the TSI

We observed a change in the radiative properties of the network pattern identified along the ascending phase of Solar Cycle 23, so we tried a first-order evaluation of the network contribution to the TSI cycle variation using a simple black-body model. We assumed that the continuous radiation of the photospheric network and internetwork regions corresponds to those of black-bodies with the network at a slightly increased brightness temperature. This assumption is done to estimate the $\delta T/T$ corresponding to the measured network contrast changes.

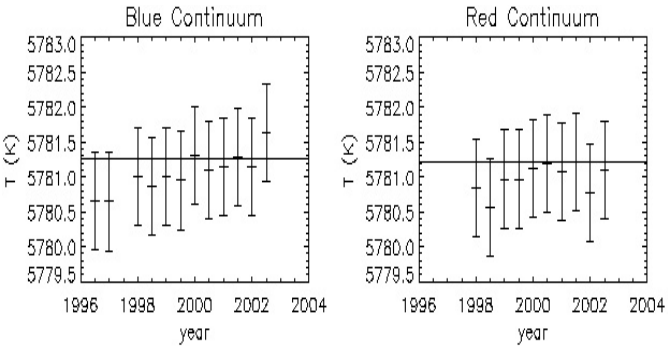

Fig. 5. Temporal variation of the network brightness temperature in the two continuum bands over the period analyzed, spanning the ascending phase of Solar Cycle 23, from July 1996 to September 2002. Comparison with the network brightness temperature corresponding to the network contrast (line) computed with a semiempirical atmospheric model of the network features (Penza et al. 2003a). Bars represent the error of the value computed by the propagation error theory in each bin.

Making such an assumption, the continuum intensity contrast is described by:

$$\frac{I^{\lambda}_{\rm Net}}{I^{\lambda}_{\rm quiet}} = C_{\lambda} = \frac{B\left(\lambda, T_{\rm Net}\right)}{B\left(\lambda, T_{\rm quiet}\right)}$$

where $B(\lambda, T)$ is the Planck function computed at the wavelength λ and temperature T, C_{λ} is the intensity contrast at the wavelength λ, I is the solar intensity at the wavelength λ for network and quiet Sun regions.

We assumed a temperature of 5780 K (Phillips 1999) for the quiet Sun and used the values for the network contrast reported in Fig. 4. We obtained the network brightness temperature changes in the blue and in the red continua shown in Fig. 5.

We then described the total solar irradiance flux $F^{\lambda}_{\rm TOT}$ by

$$F^{\lambda}_{\rm TOT} = (1-\alpha)\, B\left(\lambda, T_{\rm Sun}\right) + \alpha B\left(\lambda, T_{\rm Net}\right).$$

We assumed a constant temperature excess for the network over the solar disk and used the computed percentage of network disk coverage α to evaluate the power ΔS emitted by the whole network pattern.

The network contribution to TSI cycle variation

$$\frac{\Delta S}{S} \approx \frac{4\alpha\delta T_{\rm eff}}{T_{\rm quiet}}$$

is $\simeq 3$–4×10^{-4} (in red and blue bands) assuming the temporal variation of the network properties obtained for the whole period analyzed (Fig. 6).

6. Discussion

The radiative output of the Sun is modulated by the solar activity as an effect of the appearance of dark and bright magnetic features on the solar disk (see for example Lean 1997). We focused on the measurement of quiet network variations over the activity cycle and to the evaluation of the fraction of TSI variations due to the network pattern alone. We analyzed photometric full-disk observations carried out to support solar irradiance studies and developed appropriate procedures to automatically identify the low contrast, fine network pattern on these full-disk images.

6.1. The network identification

Network regions were identified on CaII K images by applying automated pattern recognition methods. We assumed a link existing between CaII K intensity and magnetic field (Skumanich et al. 1975) to identify the magnetic solar feature believed responsible for long-term TSI variation. We also assumed that continuum and CaII K identified features have essentially identical extent. Really, we should take into account that corresponding photospheric and chromospheric magnetic features occur at different heights in the solar atmosphere, being co spatial but with a finer structure in the photosphere than their relatively coarse structure in the chromosphere (Chapman & Sheeley 1968). Our estimate of the TSI network contribution involves the product of area times brightness excess. We consider that the larger chromospheric network includes the lower photospheric one. Thus, the photospheric contrast measured will tend to underestimate the true contrast value, while the identification method tends to overestimate the network photospheric disk coverage. To tackle this problem we compared the center to limb variation of the network contrast over the disk found by the present study with that calculated through the semiempirical model of the corresponding magnetic feature proposed by Fontenla et al. (1999), specially synthetized for the two continuum PSPT bands of observation (Penza et al. 2003a). The difference between the computed and the experimental CLV of the network contrast is less than 0.05% until $\mu \approx 0.3$, properly taking into account a "dilution" effect of the network identification with the quiet Sun at the various disk positions.

Moreover, we applied the whole analysis to simulated images of the Sun in order to test its capability of identifying the network pattern in the CaII K images, as well as its capability of measuring the network properties in the continuum and the CaII K images.

The simulated images of the Sun were obtained superimposing a network grid pattern on a quiet Sun intensity surface described through the Pierce & Slaughter (1977) coefficients. We assumed that the network disk coverage was $\alpha = 0.15$, the network contrast in the chromosphere was $C_K = 0.6\%$ and in the photosphere $C = 0.04\%$. We described the photonic noise with a Gaussian noise proportional to the square root intensity. Applying the identification procedure, our analysis gives: $\alpha = 0.15$, $C_K = 0.7\%$ and $C = 0.04\%$.

We also verified the statistical significance of the method by applying a test analysis on a sample of 512×512 pixel subarrays extracted at the disk center of the original PSPT images. In particular, we considered:

1) superimposed calculated patterns and original images taken on different days;
2) superimposed shifted pattern (1 and 3 pixels) and original images taken on the same day;
3) randomly selected pixels on original images taken on the same day.

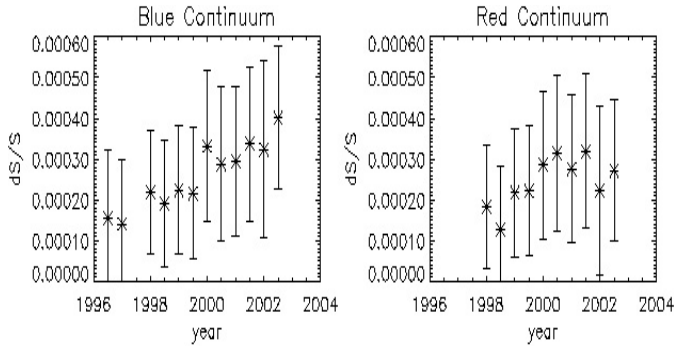

Fig. 6. Temporal variation of the estimated network contribution to TSI over the period analyzed, spanning the ascending phase of Solar Cycle 23, from July 1996 to September 2002. Bars represent the error of the value computed by the propagation error theory in each bin.

The values of the network contrast we computed are statistically significant only for superimposing the 1 pixel shifted pattern on the corresponding original images. This result suggests that the pattern identified by the method (actually) corresponds to the bright pattern both on CaII K and on continuum images, within the 1 pixel shift.

6.2. The network properties: Comparison to previous research

By applying our analysis we obtained a measure of contrast and disk coverage of the network pattern identified both in the photosphere and in the chromosphere. We found that, at the disk center, the photospheric network contrasts are only a few tenths of a percent in the two continuum PSPT bands; instead, the chromospheric network contrast in the CaII K band is a few units of a percent.

The comparison of the results we obtained with those already presented in the literature is not a straightforward exercise. As a rule, the results already presented are a consequence both of the method of analysis usedand of the quality of the observations analyzed (including wavelength, passband and spatial scale), as well as by the method used to identify the network pattern. In the past, the latter was mainly by visual selection.

Beckers (1968) obtained a network contrast of ≃0.3% with broad-band continuum images centered at 4850 Å. Frazier (1970) found 1% contrast on 4850 Å. Liu (1974) used time averaging techniques on white light images to obtain images of the network at the disk center. However, the contrast was not measured. Other monochromatic studies found 0.29% at 5265 Å (Skumanich et al. 1975), 0.1% at 5256 Å (Foukal & Fowler 1984). Lin & Kuhn (1992) found a root-mean-square amplitude (rms) of the contrast at disk center of $(2.34 \pm 0.38) \times 10^{-3}$ and $(1.83 \pm 0.51) \times 10^{-3}$ respectively for the broad-band (10 nm FWHM) green (500 nm) and red (650 nm) continuum.

More recently, Ortiz et al. (2002a) presented the active region faculae and network continuum contrast dependence on the disk and the measured magnetic signal as obtained analyzing MDI/SOHO images. They found that the CLV of the continuum contrast of magnetic features changes gradually with magnetogram signal (or magnetic filling factor), such that the contrasts of active region faculae and network exhibit a very different CLV. In particular, they found that the network feature shows a low and almost constant contrast, as compared to the pronounced CLV of the contrast for active region faculae. They measured a network contrast at the disk center ≤0.01 for the MDI continuum band.

The results we obtained are consistent with the earlier measure reported by Skumanich et al. (1975). In fact, we found a network contrast at the disk center of about 0.15% in the blue continuum PSPT band, with a network disk coverage ≈0.38 at the activity maximum, while Skumanich et al. reported a monochromatic contrast of 0.34% at 5265 Å, with a network disk coverage 0.39 by analyzing observations taken in 1968, that correspond to an activity maximum, with a spatial scale comparable to that of the PSPT observations.

About the chromospheric network contast, the comparison of the results obtained with those already presented in the literature is still not direct. In fact, previous research was based on the analysis of spectroheliograms observations (White & Suemoto 1968; Skumanich et al. 1975) that undoubtedly represent different atmospheric layers with respect to those observed through the PSPT CaII K interference filter. We obtained a contrast at the disk center ≈3.6%, that is close to the ≈4.2% noticed by White & Suemoto (1968).

6.3. The network properties: Variation in time

The network pattern has been already observed to change with solar activity. However, only sparse results exist in the literature, mainly concerning variations of the chromospheric pattern.

Sheeley (1967) noted that the chromospheric network appears "wider and more complete" at the time of sunspot maximum than at minimum. Tsap & Laba (1973), as well as Dara & Macris (1980), studied the variation of the chromospheric network over Solar Cycle 19. They found that the brightness of the chromospheric network changes with solar activity. Caccin et al. (1998) also found variations of the chromospheric network radiative properties by analyzing spectroheliograms obtained over two solar cycles. More recently, Ortiz et al. (2002b) started to study variations of the photospheric network contrast during the rising phase of Solar Cycle 23.

Careful analyses of both the quality of the images analyzed and the telescope characteristics in time is needed to assess any temporal change of the network properties during the period analyzed.

Given the technical details of the telescope, the database obtained with the PSPT is certainly unique for what concern photometric accuracy and continuity. Nevertheless, the real quality of the Rome-PSPT data, with particular regard to photometric accuracy, spatial scale and scattered light level, has been carefully evaluated analyzing the full archive of observations. Summarizing the results discussed by Fazzari et al. (2003), a substantial fraction of the database is composed of particularly high quality images (i.e. about 2 arcsec spatial resolution and 0.1% pixel photometric accuracy), as required to measure small variations in the mean thermodynamic stratification of the solar atmosphere. A seasonal variation of the data

quality resulted, probably due both to an image defocusing on the camera and to the local seasonal variation of the sky transparency.

The analysis of the quality of the images selected to perform the study presented shows a long-term small change of only one image quality. In particular, we report a long-term change of the scattered light level in the images, besides the seasonal variation of the image scale already cited. Both these variations should not be responsible for the cycle variation of the network radiative properties presented here, but are responsible for a dilution effect of the identified feature that should determine for example a decrease of the network contrast over time.

The telescope characteristics were accurately calibrated and monitored, the main aim of the study being the measure of any temporal variation of the faint network photometric properties. In brief (Centrone et al. 2002a,b), the camera gain is fully comparable to that specified by the camera constructors, but the camera read out noise is 2× larger close to the reading saturation, while comparable ($\approx 50e^-$) to that specified ($\approx 40e^-$) at lower intensity reading regimes. Note that the photonc noise dominates the data acquisition and a small increase of the camera read out noise cannot cause a trend in the temporal variation of the network photometric properties. The interference filter transmission profiles are very stable to variations of the filter temperature, with the transmission profiles centered on the specified central wavelengths and band-pass.

6.4. The network contribution to TSI

The evaluation of the network contribution to TSI cycle variation we presented is based on measured changes to network properties obtained analyzing images acquired in a seven years period during the ascending phase of Solar Cycle 23. There are a number of "constraints" in our evaluation. First, our evaluation is based on the results presented that are strongly characterized by the spatial resolution and the photometric accuracy of the data analyzed, together with the accuracy of the applied image processing. As already discussed, we performed several tests of the accuracy of the measurements. Another constraint in our evaluation is that we have measured the variation of network properties avoiding, with redundance, the enhanced bright pattern surrounding active regions. Thus the change derived here tends to estimate the contribution of the pattern usually quoted in the literature as the quiet magnetic network pattern. However, the redundant masking of bright patterns performed cannot get rid of the physical processes responsible for the appearance of the network itself, i.e. magnetic flux tube remnants of dispersed bright active regions, as well as of spots, collect at the cell boundaries as a result of the sweeping action of supergranulation flows. We are aware that the distribution of bright magnetic features on the solar disk is a continuous one at the different spatial scales and that all magnetic features on the solar disk, independently of their scale, contribute to TSI. We are now working to merge the results obtained by evaluating bright and dark active region contributions to TSI to those obtained in the present work. In particular, we are using semiempirical atmospheric models of these three classes of solar magnetic features together with the image analysis results to study TSI variations and their relationship to the magnetic field on the solar disk (Penza et al. 2003b).

The most important constraint in our evaluation is that we assume the quiet Sun and the network pattern radiate as blackbodies with the network at a slightly elevated temperature. This simple approach can be used only to evaluate the overall contribution to the total energy, while sophisticated models are needed to describe the contribution in particular spectral regions (for example, UV).

The assumed constant temperature excess over the solar disk means an invariance of the network contrast at the various μ values. The analysis of full-disk images confirms this assumption with an accuracy of the order of 1×10^{-3} for $1 \leq \mu \leq 0.2$. This result is essentially in agreement with that presented by Ortiz et al. (2002a) for the center to limb variation of the continuum contrast of small magnetic features identified in MDI images. However, note that taking into account the geometrical projection effect occurring at the various disk positions we report an increase of the network contrast toward the disk limb.

In the present analysis we report a network disk coverage change over the period analyzed of the order of 6% together with a change of about 0.05% of the network contrast in the two PSPT continuum bands. The disk coverage change we found is in good agreement with that noticed by Foukal et al. (1991).

Assuming a network disk coverage change over the solar cycle of the order of 6% together with a constant network brightness excess temperature (Berrilli et al. 1999a), we obtained an evaluation of the network contribution to TSI variations $<5 \times 10^{-5}$. However, the present analysis pointed out also a change in the network contrast that has to be taken into account. With this change, the network contribution to TSI over the cycle becomes $\approx 3\text{–}4 \times 10^{-4}$.

Note that the change in the network contrast has a much larger contribution to the TSI variation than the change in the network disk coverage. So, our analysis suggests that the disk coverage increase is less significant for the computation of the irradiance contribution than the contrast increase.

The TSI change given by the measurements performed by VIRGO on board SOHO during the period analyzed results is $\approx 7.5 \times 10^{-4}$ by the most recent version of the TSI measure (version 5-006-0305) provided by the Physicalisch-Meterologisches Observatorium Davos World Radiation Center, Davos Switzerland.

7. Conclusions

We evaluated the contrast and disk coverage of the network defined by the photospheric counterpart of the chromospheric network. This was identified on CaII K images through automated procedures that use skeletonizing algorithms. The results of our analysis were obtained by direct superimposition of the identified chromospheric network pattern on continuum photospheric images.

We found a brightness excess of the photospheric network contrast with respect to the quiet Sun on the whole solar disk. The contrast values obtained from continuum and CaII K

images are in agreement with some earlier evaluations reported in the literature.

We then studied the temporal variation of both the network contrast and the disk converage over a seven years period corresponding to the ascending phase of the current solar cycle. We found a change of both the radiative properties. In particular, we saw a change of the order of 6% of the disk coverage and a change of about 0.05% in the contrast in the two continuum PSPT bands.

By assuming that the network continuum contrast variations are due to an enhancement of the brightness temperature of the corresponding region of the solar surface we obtained a change of the temperature excess for the network with respect to the quiet Sun of the order of $\Delta T \simeq 0.5$ K along the period analyzed.

We evaluated a network contribution to TSI of the order of $3{-}4 \times 10^{-4}$ over the cycle.

In the present study we show that the contribution of the quiet network to long-term irradiance variation needs to be taken properly into account when modeling variations of TSI.

Acknowledgements. I.E. would like to thank M. Centrone and F. Giorgi for carefully calibrating the Rome-PSPT telescope characteristics, as well as useful comments by B. Caccin, V. Penza and G. de Toma that led to substantial improvements of the study presented. The authors acknowledge unpublished data from the VIRGO experiment on the cooperative ESA/NASA Mission SOHO, always assumed as reference for the knowledge of TSI variations over the current solar cycle, during the very long development of this study.

References

Beckers, J. M. 1968, Sol. Phys., 5, 309
Berrilli, F., Florio, A., & Ermolli, I. 1998, Sol. Phys., 180, 29
Berrilli, F., Florio, E., & Ermolli, I. 1999a, IUGG, Abstracts, A, 88
Berrilli, F., Ermolli, I. Florio, A., & Pietropaolo, E. 1999b, A&A, 344, 965
Caccin, B., Ermolli, I. Fofi, M., & Sambuco, A. M. 1998, Sol. Phys., 177, 295
Centrone, M., Giorgi, F., & Ermolli, I. 2002a, Technical Report Rome Observatory, 02-S1
Centrone, M., Giorgi, F., & Ermolli, I. 2002b, Technical Report Rome Observatory, 02-S2
Chapman, G. A., Cookson, A. M., & Dobias, J. J. 1996, J. Geophys. Res., 101, 13541
Chapman, G. A., & Sheeley, N. R. Jr. 1968, Sol. Phys., 5, 442
Coulter, R. L., & Kuhn, J. F. 1994, in Active Region Evolution: Comparing Models with Observations, ed. K. S. Balasubramaniam, & G. W. Simon, ASP Conf. Ser., 68, 37
Dara, H. C., & Macris, C. J. 1980, Bull. Astron. Inst. Czechosl., 31, 364
de Toma, G., White, O. R., Knapp, B. G., Rottman, G. J., & Woods, T. N. 1997, J. Geophys. Res., 102, 2597
de Toma, G., White, O. R., Chapman, G. A., et al. 2001, ApJ, 549, L131
Ermolli, I., Fofi, M., Bernacchia, C., et al. 1998a, Sol. Phys., 177, 1
Ermolli, I., Fofi, M., & Torelli, M. 1998b, Mem. SAIt., 69, 587
Ermolli, I., Centrone, M., & Fofi, M. 2001, Mem. SAIt., 72, 673
Fazzari, C., Ermolli, I., Centrone, M., Giorgi, F., & Criscuoli, S. 2003, Mem. SAIt., in press
Fligge, M., Solanki, S. K., & Unruh, Y. 2000, A&A, 353, 380
Florio, A., & Berrilli, F. 1998, Mem. SAIt., 69, 655
Fontenla, J., White, O. R., Fox, P. A., Avrett, E. H., & Kurucz, R. L. 1999, ApJ, 518, 480
Foukal, P., & Fowler, L. 1984, ApJ, 281, 442
Foukal, P., & Lean, J. 1988, ApJ, 328, 347
Foukal, P., Harvey, K., & Hill, F. 1991, ApJ, 383, L89
Frazier, E. N. 1970, Sol. Phys., 14, 89
Fröhlich, C. 1994, The Sun as a variable star, ed. J. Pap, C. Fröhlich, H. S. Hudson, & S. Solanki (Cambridge Univ. Press), IAU Colloq., 143, 28
Fröhlich, C., & Lean, J. 1998, Geophys. Res. Lett., 25, 4277
Fröhlich, C. 2000, Space Sci. Rev., 94, 15
Hagenaar, H. J., Schrijver, C. J., & Title, A. M. 1997, ApJ, 481, 988
Harvey, J. W., & Livingston, W. C. 1994, Infrared solar physics, ed. D. M. Rabin, J. T. Jefferies, & C. Lindsey, Dordrecht, IAU Symp., 154, 59
Harvey, K. L., & White, O. R. 1999, ApJ, 515, 812
Johannesson, A., Marquette, W. H., & Zirin, H. 1998, Sol. Phys., 177, 265
Jones, H. P., Branston, D. D., Jones, P. B., & Popescu, M. D. 2003, ApJ, 589, 658
Krivova, N. A., Solanki, S. K., Fligge, M., & Unruh, Y. C. 2003, A&A, 399, L1
Kuhn, J. R., Libbrecht, K. G., & Dicke, R. 1985, Science, 213, 957
Kuhn, J. R., Bush, R., Scherrer, P., & Scheick, X. 1998, Nature, 392, 155
Kuhn, J. R., Lin, H., & Loranz, D. 1991, PASP, 103, 1097
Lean, J. 1997, ARA&A, 35, 33
Li, L., & Sofia, S. 2001, ApJ, 549, 1204
Lin, H., & Kuhn, J. R. 1992, Sol. Phys., 141, 1
Liu, S. 1974, Sol. Phys., 39, 297
Ortiz, A., Solanki, S. K., Domingo, V., Fligge, M., & Sanahuja, B. 2002a, A&A, 388, 1036
Ortiz, A., Domingo, V., Sanahuja, B., & Solanki, S. K. 2002b, ESA-SP, 508, 185
Phillips, A. C. 1999, The Physics of the stars (Wiley)
Penza, V., Caccin, B., Ermolli, I., & Centrone, M. 2003a, A&A, submitted
Penza, V., Caccin, B., & Ermolli, I. 2003b, in preparation
Pierce, A. K., & Slaughter, C. D. 1977, Sol. Phys., 51, 25
Preminger, D. G., Walton, S. R., & Chapman, G. A. 2001, Sol. Phys., 202, 53
Skumanich, A., Smythe, C., & Frazier, E. N. 1975, ApJ, 200, 747
Sheeley, N. R. Jr. 1967, Sol. Phys., 1, 171
Sofia, S. 1998, Sol. Phys., 177, 413
Tsap, T. T, & Laba, I. S. 1973, Izv. Krymsk. Astrofiz. Obs., 48, 73
Turmon, M., Pap, J. M., & Mukhtar, S. 2002, ApJ, 568, 396
Ulrich, R. K., & Bertello, L. 1995, Nature, 377, 214
Willson, R. C., Hudson, H. S., Fröhlich, C., & Brusa, R. 1986, Science, 211, 708
White, O. R., & Suemoto, Z. 1968, Sol. Phys., 3, 523
Worden, J. R., White, O. R., & Woods, T. N. 1998, ApJ, 496, 998